Design and Analysis of Cable-Driven Parallel Robot *CaRISA*: a Cable Robot for Inspecting and Scanning Artwork

Philipp Tempel[1], Matthias Alfeld[2], and Volkert van der Wijk[1]

[1] Delft University of Technology, Department of Precision and Microsystems Engineering, Mekelweg 2, 2628 CD Delft, The Netherlands p.tempel@tudelft.nl
[2] Delft University of Technology, Department of Materials Science and Engineering, Mekelweg 2, 2628 CD Delft, The Netherlands

Abstract. Cultural heritage science envisages understanding of methods and techniques used by past painters and sculptors in creating their masterpieces of art. Existing devices for in situ and non-destructive, automated scanning are large and bulky and built around the assumption of a perfectly planar surface. We are developing a lightweight, portable robot for scanning of paintings, marbles, or statues while explicitly allowing for their out-of-plane surface. This paper presents the kinematic design and analysis of the wrench-feasible workspace of a cable-driven parallel robot capable of positioning an imaging device with three translational and two rotational degrees of freedom. At the end stand geometric parameters optimized for the application requirements allowing for pan and tilt of 70° each in total, making scanning of the spatial surface of art objects possible.

Keywords:
cable-driven parallel robot · geometric design · workspace analysis

1 Introduction

Cultural heritage science aims at deeply understanding cultural heritage objects which necessitates knowledge of its material character reflecting creation and history. Insight is commonly acquired by means of imaging techniques such as X-ray fluorescence imaging or reflectance imaging spectroscopy for the identification of chemical properties which can reach every layer of paint of an image, even those below the visible surface. Attribution of paintings to famous artists e.g., Vincent van Gogh is one use case [3], preservation for future generations another. Given the heterogeneity of a cultural heritage object, it is often not sufficient to investigate selected spots, but to scan a significant part of the object [4].
Frequently employed techniques are derived from laboratory setups for the investigation of planar samples. However, artists purposefully create paintings with topographical surface to provide a level of plasticity and depth. This is particularly interesting for painted marbles from Roman or Greek antiquity [2, 7] where correction for variation in the surface was made in post processing. However, not all image distortion is recoverable and may more easily be avoided when capturing an image.
Common devices are handheld, or tripod-mounted or table-mounted. Handheld operation limits the analysis to isolated spots and, consequently, does not allow for

Fig. 1: CAD rendering of proposed cable robot CaRISA depicted scanning Vermeer's *Girl with a Pearl Earring* (picture CC-BY-SA 3.0 Unported License).

acquisition of representative data. Tripod-mounted devices can be positioned more freely and can, to some extent, account for surface curvature, yet their scanning range is only a few hundred square centimeters [6]. Table-mounted devices allow for scanning large areas, and, in some cases, can also follow the surface to keep a constant distance, however, the measurement head cannot be panned or tilted [17]. Panning and tilting the view is needed to uncover shaded areas and to keep the plane of focus aligned.

All operated systems provide for serial motion of the imaging device, resulting in terminal positioning inaccuracy due to error accumulation of each axis. Using a parallel kinematic manipulator can remedy this disadvantage since the terminal accuracy is not determined by only a single axis' error. However, they feature a workspace much smaller than their footprint due to limited axis stroke. Replacing the m rigid link actuators with elastic and flexible cables can drastically increase the workspace of the parallel robot yet compromises accuracy and stiffness.

A cable-driven parallel robot (cable robot) nevertheless seems appropriate for this type of application due to its large workspace and scalable design. To the best of the authors' knowledge, only two types of cable robots have been developed for carrying an imaging device. The most well-known system is SkyCam by Cone et al. [5], displacing a camera for aerial view of sports matches. Gosselin et al. developed a cable robot for capturing the appearance of objects using 6-degree of freedom (DoF) with a 1-DoF gravity-powered passive mechanism end effector displacing a high resolution camera on a hemisphere centered around the object [8]. Practicality of cable robots for scanning art has yet to be investigated.

In this contribution, we present a Cable Robot for Inspecting and Scanning Artwork (CaRISA) (see Figure 1) of non-planar, spatial objects alike to paintings and frescos. Our robot is designed to be used in situ i.e., it is deployed on-site of the artwork and arranges itself around the piece of art. Our resulting robot is novel in that we are providing the application-optimal geometric design for the task of scanning artwork in the general realm of paintings.

This paper is structured as follows: Section 2 presents the application and hardware requirements from which we infer the cable robot properties and archetype design in Section 3. Succeeding is the workspace analysis in Section 4 showing the

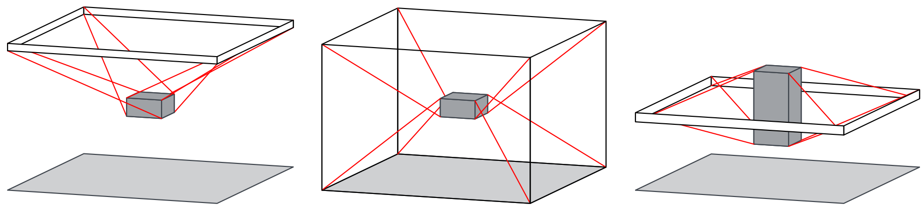

(a) Suspended: cables routed upwards from the platform.

(b) Constrained: cables routed up- and downwards from the platform.

(c) Protruding: thin frame with platform protruding from it.

Fig. 2: Schematic drawings of (a) suspended, (b) fully constrained, and (c) protruding designs.

used kinematics model as well as the obtained application-optimal final geometry. Section 5 summarizes and concludes the paper.

2 Application Requirements and Specification

We assume the artwork to be a three-dimensional surface over which the imaging device is moved subsequently capturing the whole piece. The positioning device must allow for keeping the optical axis aligned with the scanning area normal. This results in a 5-DoF workspace: 3 translational DoF and 2 rotational DoF for panning and tilting. The spatial extent of the workspace clearly depends on painting size and focal range of the imaging device. We assume it to be (80×60) cm in width and height, the size also covered by established instruments. Panning and tilting must be possible for the range of $(-35 \text{ to } 35)^\circ$, similar to existing devices with only tilting ability.

CaRISA is equipped with a Dino-Lite Digital Microscope camera offering imaging in visible and invisible light (UV and IR). The camera is attached to a DinoLite WF-10 WiFi Streamer, providing power over USB and wireless data transmission. The cable robot operates by capturing an image when at rest, thus no live data feed is needed. With a focal distance ranging from 22 mm to 48 mm, the camera has a maximum field of view of 70°. The camera's CMOS chip features (1280×1024) px giving an image pixel size of 10 µm to 15 µm.

In situ scanning of the art object implies it be left at its location of installation and the positioning and imaging device being fitted around. As such, the device must be mobile, transportable, adjustable, and allow for scanning outside of its footprint.

3 Structural Design

A cable robot consists of a mobile platform with n DoF driven by m cables. Verhoeven et al. [18] categorize them by their redundancy $r = m - n$ as i) underactuated or incompletely restrained when $m \leq n$, ii) completely restrained when $m = n + 1$, and iii) overactuated or redundantly restrained when $m > n + 1$. Either category can be operated either suspended i.e., crane-like (CoGiRo [9], Figure 2(a)), or (fully) constrained (SEGESTA [11], Figure 2(b)). While crane-like cable robots are unable to withstand all external wrenches and some DoF may be uncontrollable, fully constrained systems can balance arbitrary wrenches and have all DoF

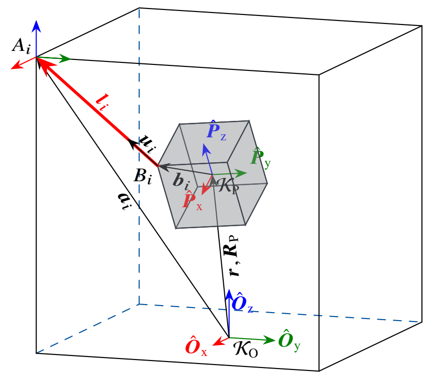

Fig. 3: Kinematic robot model with world coordinate system $\mathcal{K}_O = (O; \hat{\boldsymbol{O}}_x, \hat{\boldsymbol{O}}_y, \hat{\boldsymbol{O}}_z)$ and local platform coordinate system $\mathcal{K}_P = (P; \hat{\boldsymbol{P}}_x, \hat{\boldsymbol{P}}_y, \hat{\boldsymbol{P}}_z)$.

controllable. Inherent to most cable robots is a small orientation workspace due to cable-cable collision or infeasibility of attaining static equilibrium. CoGiRo's special design allows for large rotation of more than 100° around one axis [9].
A third, rarely used archetype is the protruding FALCON7-design by Kawamura et al. [12]. It features a thin frame out of which the platform protrudes (see Figure 2(c)). The design was intended for high-speed pick-and-place applications requiring high stiffness, achieved by the out-of-plane cable connections. Besides allowing for a large orientation workspace, this also results in the workspace being located outside of the frame. Given the limitations of a workspace-enclosing design or a crane-like design, choosing the FALCON7-design implies itself.

4 Workspace Analysis

The tool center point (TCP) must reach every point within a cuboid of dimensions $(80 \times 10 \times 60)$ cm, the depth of 10 cm chosen to allow also using other imaging devices in a later stage.

4.1 Kinematics Model

We assume the standard kinematic model (cf. Figure 3) as originally presented by Albus et al. [1], where the mobile platform is positioned at $\boldsymbol{r}$ with orientation $\boldsymbol{R}_P = \boldsymbol{R}_{\hat{\boldsymbol{P}}_x}(\alpha)\,\boldsymbol{R}_{\hat{\boldsymbol{P}}_z}(\gamma)$, pan and tilt; rotation about focal axis $\hat{\boldsymbol{P}}_y$ is of no interest. A vector loop is drawn from the i-th frame anchor A_i at $\boldsymbol{a}_i$ and attached to the ith platform anchor B_i at $\boldsymbol{b}_i$ w.r.t. the platform coordinate system $\mathcal{K}_P$. This yields the cable length from

$$L_i = \|\boldsymbol{l}_i\| = \|\boldsymbol{a}_i - (\boldsymbol{r} + \boldsymbol{R}_P \boldsymbol{b}_i)\|\,.$$

Static equilibrium of the cable robot can be achieved by balancing all m cable forces f_i with the external wrench $\boldsymbol{w}$ such that it reads

$$\boldsymbol{A}^\top \boldsymbol{f} + \boldsymbol{w} = \begin{bmatrix} \boldsymbol{u}_1 & \dots & \boldsymbol{u}_m \\ \boldsymbol{b}_1 \times \boldsymbol{u}_1 & \dots & \boldsymbol{b}_m \times \boldsymbol{u}_m \end{bmatrix} \begin{bmatrix} f_1 \\ \vdots \\ f_m \end{bmatrix} + \boldsymbol{w} = \boldsymbol{0}\,, \tag{1}$$

Table 1: Final geometric positions of each cable frame anchor $\boldsymbol{a}_i$ and platform anchor $\boldsymbol{b}_i$.

	Frame anchor			Platform anchor		
Cable	$\boldsymbol{a}_{i_\mathrm{x}}$/m	$\boldsymbol{a}_{i_\mathrm{y}}$/m	$\boldsymbol{a}_{i_\mathrm{z}}$/m	$\boldsymbol{b}_{i_\mathrm{x}}$/m	$\boldsymbol{b}_{i_\mathrm{y}}$/m	$\boldsymbol{b}_{i_\mathrm{z}}$/m
1	−1.250	0.100	1.250	−0.075	0.075	−0.075
2	1.250	0.100	1.250	0.075	0.075	−0.075
3	1.250	−0.100	1.250	0.075	0.775	−0.100
4	−1.250	−0.100	1.250	−0.075	0.775	−0.100
5	−1.250	0.100	−0.750	−0.075	0.050	0.075
6	1.250	0.100	−0.750	0.075	0.050	0.075
7	1.250	−0.100	−0.750	0.075	0.800	0.100
8	−1.250	−0.100	−0.750	−0.075	0.800	0.100

with the cable direction vector $\boldsymbol{u}_i = \boldsymbol{l}_i / L_i$. Above equation describes the *structure equation* with the *structure matrix* $\boldsymbol{A}^\top$ [10], and at the core of determining the wrench-feasible workspace (WFW). Even though pulleys are used for guiding the cables, we neglect them in the analysis since their influence on the workspace space is negligibly small for the robot dimensions (see [13] for a discussion).

4.2 Workspace Archetype and Criterion

The TCP shall be positioned in the spatial extent of the cuboid in front of the painting (cf. Section 2) such that any orientation within the set of possible rotations can be attained. This total orientation workspace

$$\mathcal{W}_\mathrm{TO}(\mathcal{R}) = \{\boldsymbol{r} \in \mathbb{R}^3 \mid \hat{\boldsymbol{y}} = \langle \boldsymbol{r}, \boldsymbol{R}_\mathrm{P} \rangle \, \forall \, \boldsymbol{R}_\mathrm{P} \in \mathcal{R}\},$$

is the set of poses which contains all positions $\boldsymbol{r}$ where all orientations $\boldsymbol{R}_\mathrm{P}$ are in a given set of orientations $\mathcal{R}$. Pose validity is checked based on wrench-feasibility i.e., checking if there exists a force distribution $\boldsymbol{f}_\sim \in [\boldsymbol{f}_-, \boldsymbol{f}_+] = [10\,\mathrm{N}, 150\,\mathrm{N}]$ such that Equation (1) holds true. Since the platform must not touch the artwork, the external wrench $\boldsymbol{w} = m_\mathrm{P} \cdot [\boldsymbol{g}^\top, (\boldsymbol{R}_\mathrm{P}\, \boldsymbol{\varrho} \times \boldsymbol{g})^\top]^\top$ comprises only gravitational forces and torques, with total platform mass $m_\mathrm{P} = 5\,\mathrm{kg}$, direction of gravity $\boldsymbol{g} = [0, 0, -g]^\top$, and the center of gravity (CoG) $\boldsymbol{\varrho}$ in platform coordinates. We solve Equation (1) using the Improved Closed-Form by Pott [14], which solves

$$\boldsymbol{f}_\sim = \bar{\boldsymbol{f}} - \boldsymbol{A}^{\top+} (\boldsymbol{w} + \boldsymbol{A}^\top \bar{\boldsymbol{f}}),$$

where $\bar{\boldsymbol{f}} = (\boldsymbol{f}_+ + \boldsymbol{f}_-)/2$. If no force distribution can be found, the pose is not within the WFW.

4.3 Application-Optimal Workspace

Our design goal is to find a set of dimensions for frame and mobile platform such that CaRISA covers the whole painting area for all focal distances. As any arbitrarily large configuration will cover the volume of interest, we search for those satisfying additional constraints on the platform shape and maximum frame dimensions. Through gradient-based methods we find a locally optimal solution to the non-linear constrained optimization problem (see methods in [15]).
The final frame and platform dimensions are given in Table 1, which shows cable attachment in a crosswise sequence, yet cable-cable collision does not occur in

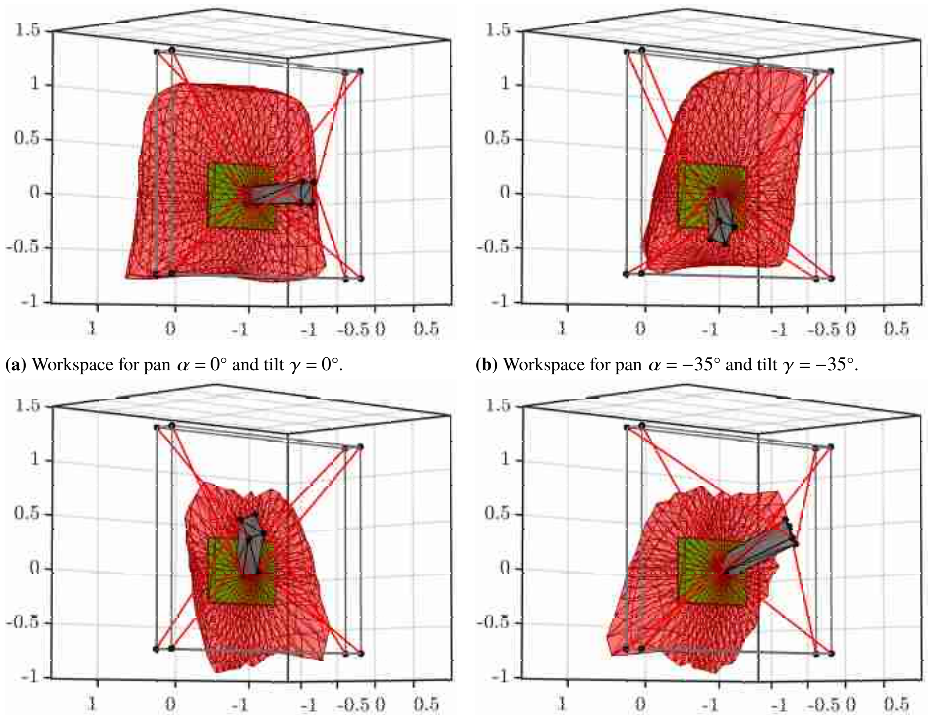

(a) Workspace for pan $\alpha = 0°$ and tilt $\gamma = 0°$.

(b) Workspace for pan $\alpha = -35°$ and tilt $\gamma = -35°$.

(c) Workspace for pan $\alpha = 35°$ and tilt $\gamma = -35°$.

(d) Workspace for pan $\alpha = 35°$ and tilt $\gamma = 35°$.

Fig. 4: Translation wrench-feasible workspace for multiple orientations of the platform.

the volume of interest. Figure 4 shows the workspace for multiple orientations of the mobile platform to account for the desired range of pan and tilt. All figures show the desired workspace in light green, the platform in dark gray, the cables in red, and the obtainable translational workspace for each rotation value.

The translational workspace for rotations about $\hat{\boldsymbol{e}}_x$ or $\hat{\boldsymbol{e}}_z$ close to zero covers almost 90 % of the robot's frame area. For maximum angles of pan and tilt, coverage reduces to approximately 45 %. In either case, however, the desired volume is still within the translational WFW. For large positive rotation about $\hat{\boldsymbol{e}}_x$ i.e., the camera pointing downwards, and due to the TCP position not coinciding with the platform's CoG, the WFW is of much smaller size compared to negative rotations about $\hat{\boldsymbol{e}}_x$ i.e., with the camera pointing upwards. We conclude possibility of finding an application requirements-satisfying geometry for scanning of artwork.

From a theoretical point of view, accuracy and repeatability of the device are in the required range influenced only by the drive encoder and gear ratio. However, well-known physical challenges of cable robots of cable elasticity and flexibility do not allow for making a blanket statement on the obtainable terminal accuracy. As of writing, the physical prototype is being constructed. We are already developing further improvements to the system such as additional cable force sensors and absolute cable length measurement devices to combat cable elasticity and induced accuracy impairment.

We expect the final workspace size to be smaller to the analytical result for that 1) friction of pulleys and bearings is neglected but will inevitably impair the transmitted drive torque/force, and 2) the final assembly will not share the exact same geometry as determined analytically due to manufacturing inaccuracies and possible adjustments to the mechanical design. Despite that, the actual physical workspace is expected to be marginally smaller than the analytical workspace, which is why a theoretically larger workspace is generally preferred during design– see also [15] for a critical review of this fact.

5 Conclusions

We present the 5-DoF Cable Robot for Inspecting and Scanning Artwork (CaRISA) of cultural significance with a large translation and orientation workspace. Cable robots deems themselves a good choice due to their lightweight and modular design and their large workspace. Conventional cable robot designs are limited in their orientation workspace, which is why we choose the FALCON7-design. CaRISA's geometry is optimized for the application requirements of achieving a wrench-feasible workspace with panning and tilting of the imaging of 70° each, respectively.

Acknowledgments

The authors would like to thank Joris Dik (Delft University of Technology, Department of Materials Science and Engineering) for fruitful discussions and his contributions to the research. The results shown in this contribution were in parts generated using WireX, an open source software for analysis and design of cable robots [16].

References

1. Albus, J.S., Bostelman, R.V., Dagalakis, N.G.: The NIST ROBOCRANE: Originally published as "The NIST SPIDER, A Robot Crane". Journal of Research of the National Institute of Standards and Technologies **97**(3), 373–385 (1992)
2. Alfeld, M., Mulliez, M., Martinez, P., Cain, K., Jockey, P., Walter, P.: The Eye of the Medusa: XRF Imaging Reveals Unknown Traces of Antique Polychromy. Analytical Chemistry **89**(3), 1493–1500 (2017)
3. Alfeld, M., Siddons, D.P., Janssens, K., Dik, J., Woll, A., Kirkham, R., Wetering, E.: Visualizing the 17th century underpainting in Portrait of an Old Man by Rembrandt van Rijn using synchrotron-based scanning macro-XRF. Applied physics. A, Materials science & processing **111**(1), 157–164 (2013)
4. Alfeld, M., de Viguerie, L.: Recent Developments in Spectroscopic Imaging Techniques for Historical Paintings: A review. Spectrochimica Acta Part B: Atomic Spectroscopy **136**, 81–105 (2017)
5. Cone, L.L.: Skycam, an aerial robotic camera system. In: Byte Magazine. vol. 10, pp. 122–132 (1985)

6. Galli, A., Caccia, M., Alberti, R., Bonizzoni, L., Aresi, N., Frizzi, T., Bombelli, L., Gironda, M., Martini, M.: Discovering the Material Palette of the Artist: A p-XRF Stratigraphic Study of the Giotto Panel "God the Father with Angels". X-Ray Spectrometry **46**(5), 435–441 (2017)
7. Geil, E.C., Thorne, R.E.: Correcting for surface topography in X-ray fluorescence imaging. Journal of Synchrotron Radiation **21**(6), 1358–1363 (2014)
8. Gosselin, C.M., Bouchard, S.: A Gravity-Powered Mechanism for Extending the Workspace of a Cable-Driven Parallel Mechanism: Application to the Appearance Modelling of Objects. International Journal of Automation Technology **4**(4), 372–379 (2010)
9. Gouttefarde, M., Merlet, J.P., Daney, D.: Wrench-Feasible Workspace of Parallel Cable-Driven Mechanisms. In: Robotics and Automation (ICRA 2007): 2007 IEEE/RAS International Conference on. pp. 1492–1497 (2007)
10. Higuchi, T., Ming, A., Jiang-yu, J.: Application of Multi-Dimensional Wire Cranes in Construction. In: The 5th International Symposium on Robotics in Construction, pp. 661–668 (1988)
11. Hiller, M., Fang, S., Mielczarek, S., Verhoeven, R., Franitza, D.: Design, analysis and realization of tendon-based parallel manipulators. Mechanism and Machine Theory **40**(4), 429–445 (2005)
12. Kawamura, S., Choe, W., Tanaka, S., Pandian, S.R.: Development of an Ultrahigh Speed Robot FALCON Using Wire Drive System. In: Robotics and Automation (ICRA 1995): 1995 IEEE/RAS International Conference on. pp. 215–220. IEEE (1995)
13. Pott, A.: Influence of Pulley Kinematics on Cable-Driven Parallel Robots. In: Lenarčič, J., Husty, M.L. (eds.) Latest Advances in Robot Kinematics. pp. 197–204. Springer Netherlands (2012)
14. Pott, A.: An Improved Force Distribution Algorithm for Over-Constrained Cable-Driven Parallel Robots. In: Thomas, F., Pérez-Gracia, A. (eds.) Computational Kinematics, Mechanisms and Machine Science, vol. 15, pp. 139–146. Springer Netherlands (2014)
15. Pott, A.: Cable-Driven Parallel Robots: Theory and Application, Springer Tracts in Advanced Robotics, vol. 120. Springer International Publishing, Cham (2018)
16. Pott, A.: WireX: An Open Source Initiative Scientific Software for Analysis and Design of Cable-Driven Parallel Robots (2019)
17. Romano, F.P., Caliri, C., Nicotra, P., di Martino, S., Pappalardo, L., Rizzo, F., Santos, H.C.: Real-time elemental imaging of large dimension paintings with a novel mobile macro X-ray fluorescence (MA-XRF) scanning technique. Journal of Analytical Atomic Spectrometry **32**(4), 773–781 (2017)
18. Verhoeven, R., Hiller, M., Tadokoro, S.: Workspace, Stiffness, Singularities and Classification of Tendon-Driven Stewart Platforms. In: Lenarčič, J., Husty, M.L. (eds.) Advances in Robot Kinematics. pp. 105–114. Kluwer Academic Publishers (1998)